Inorganic Chemistry

Article

pubs.acs.org/IC

Bimetallic Ruthenium PNP Pincer Complex As a Platform to Model Proposed Intermediates in Dinitrogen Reduction to Ammonia

Sergio S. Rozenel and John Arnold*

Department of Chemistry, University of California, Berkeley, California 94720, United States

Supporting Information

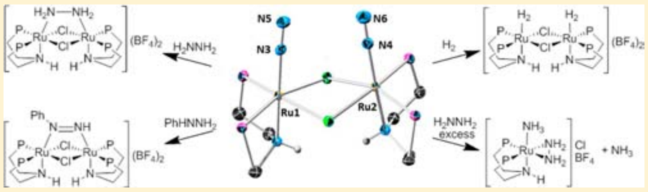

ABSTRACT: A series of ruthenium complexes was isolated and characterized in the course of reactions aimed at studying the reduction of hydrazine to ammonia in bimetallic systems. The diruthenium complex $\{[\mathrm{HPNPRu(N_2)}]_2(\mu\text{-Cl})_2\}(\mathrm{BF_4})_2$ (**2**) (HPNP = $\mathrm{HN(CH_2CH_2P^iPr_2)_2}$) reacted with 1 equiv of hydrazine to generate $[(\mathrm{HPNPRu})_2(\mu^2\text{-}\mathrm{H_2NNH_2})(\mu\text{-Cl})_2](\mathrm{BF_4})_2$ (**3**) and with an excess of the reagent to form $[\mathrm{HPNPRu(NH_3)}(\kappa^2\text{-}\mathrm{N_2H_4})](\mathrm{BF_4})\mathrm{Cl}$ (**5**). When phenylhydrazine was added to **2**, the diazene species $[(\mathrm{HPNPRu})_2(\mu^2\text{-}\mathrm{HNNPh})(\mu\text{-Cl})_2](\mathrm{BF_4})_2$ (**4**) was obtained. Treatment of **2** with H_2 or CO yielded $\{[\mathrm{HPNPRu(H_2)}]_2(\mu\text{-Cl})_2\}(\mathrm{BF_4})_2$ (**7**) and $[\mathrm{HPNPRuCl(CO)_2}]\mathrm{BF_4}$ (**8**), respectively. Abstraction of chloride using $\mathrm{AgOSO_2CF_3}$ or $\mathrm{AgBPh_4}$ afforded the species $[(\mathrm{HPNPRu})_2(\mu^2\text{-}\mathrm{OSO_2CF_3})(\mu\text{-Cl})_2]\mathrm{OSO_2CF_3}$ (**9**) and $[(\mathrm{HPNPRu})_2(\mu\text{-Cl})_3]\mathrm{BPh_4}$ (**10**), respectively. Complex **3** reacted with HCl/H_2O or HCl/Et_2O to produce ammonia stoichiometrically; the complex catalytically disproportionates hydrazine to generate ammonia.

INTRODUCTION

Achieving atmospheric nitrogen fixation to produce ammonia efficiently is one of the most challenging problems in chemistry.[1−6] Two processes account for the majority of NH_3 synthesized: the Haber and Bosch reaction and biological fixation of dinitrogen.[1−4,7−11] The former yields ammonia from dinitrogen and dihydrogen, employing an iron catalyst at high temperatures and pressures, whereas the latter occurs at ambient temperature and pressure. The most common enzyme to perform this transformation has an iron−molybdenum-sulfur cluster (the Fe−Mo cofactor) as the catalytic agent.[12,13]

Efforts have been made to explain the mechanism of nitrogen fixation via transition metal complexes.[14] The most successful experimental approaches for nitrogen reduction thus far involve a Chatt-type mechanism in which one transition metal atom coordinates N_2, and subsequent reduction generates ammonia.[15,16] However, recent studies of the Fe−Mo cofactor active site by Hoffman and co-workers favors an "alternating" pathway—where the two N atoms are hydrogenated alternately and hydrazine is formed—over a "distal" one, in which a single N atom is hydrogenated in three steps, liberating ammonia and forming a nitride species.[17]

Examples of dinitrogen reduction include the direct hydrogenation of N_2 with zirconium,[18] the reduction of hydrazine to ammonia with Fe/Mo/S cubanes[19−25] and $[\mathrm{Cp^*WMe_3}]^+$,[26,27] the oxidation of ammonia to N_2 via bridging species with Ru cofacial metalloporphyrins,[28] and the catalytic reduction of N_2 to ammonia at a single Mo center.[16] Recently, Schneider and co-workers have used a PNP-type ligand to stabilize a Ru(IV) nitrido complex that undergoes hydrogenolysis at room temperature to produce ammonia in high yield.[29] Using a related pincer ligand, Nishibayashi showed that dimolybdenum dinitrogen complexes are effective catalysts for the formation of ammonia.[15,30] Theoretical work by Qu et al. indicates that bimetallic iron complexes with sulfur bridging ligands are also capable of reducing nitrogen to ammonia, and the same group also showed the ability of this kind of diiron centers to break the N−N bond in hydrazine.[31,32]

In the nitrogenase synthesis of ammonia, it is likely that the Fe−Mo cofactor plays a bigger role in the activation of N_2 than simply acting as a single metal binding site.[12,33] Evidence indicates that the cluster acts as the binding and reducing site for N_2, as well as for the intermediates hydrazine and diazene.[10,13,34−37] Theoretical models suggest that N_2 binds to iron,[33,38] whereas recent experimental work indicates that N_2 and the hydrazine intermediate formed interact with a common 4Fe-4S face in the waist region of the cluster.[10,34,36]

Complexes with ligand frameworks that could serve to support binding of the array of potential ligands involved (nitrogen, ammonia, hydrazine, and diazene) may help us gain insights regarding nitrogenase-like activity.[39−41] Bauer and co-workers reported a ruthenium system of this type using a ethaneamine-benzenethiolate ligand,[39] and just recently, the Tyler and Peters groups described iron complexes showing analogous chemistry.[40,41] In related systems, the latter group has been able to stabilize an $\mathrm{Fe}(\eta^2\text{-}\mathrm{H_2NNH})$ complex[42] and to functionalize the N_2 ligand.[43]

In a continuation of our work using multidentate PNP-type ligands to stabilize reactive metal centers,[44,45] we turned our attention to ruthenium and have explored the chemistry of a bimetallic ruthenium system capable of supporting a series of

Received: May 17, 2012
Published: August 27, 2012

dx.doi.org/10.1021/ic3010322 | Inorg. Chem. 2012, 51, 9730−9739

Scheme 1

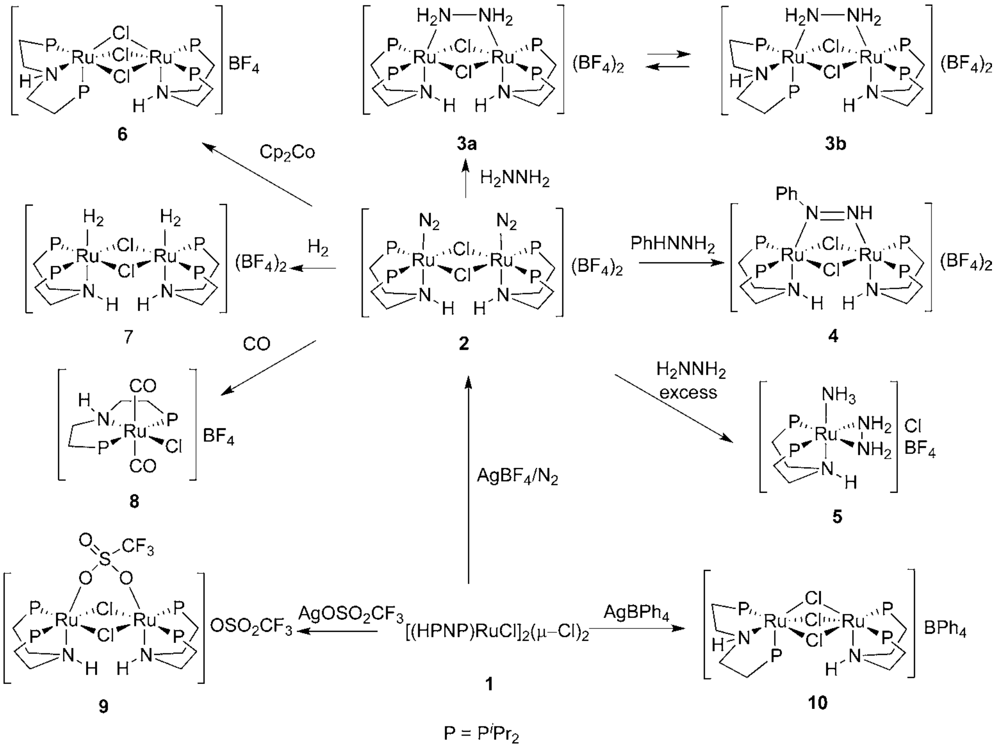

complexes with $(N_2)_2$, $(H_2)_2$, mixed N_2/H_2, diazene, and hydrazine ligands in an unusual fashion. This system also catalytically disproportionates hydrazine to produce NH_3.

RESULTS AND DISCUSSION

The starting material for our studies was the diruthenium species $(HPNPRuCl)_2(\mu\text{-}Cl)_2$ (**1**) which we prepared in a very similar manner to that described by Schneider, who was the first to report this compound.[46] Reaction of **1** with 2 equiv of $AgBF_4$ in tetrahydrofuran (THF) at room temperature under nitrogen resulted in a color change from orange to yellow and the formation of AgCl (Scheme 1). After work up of the reaction mixture, the bridging chloride complex $\{[HPNPRu(N_2)]_2(\mu\text{-}Cl)_2\}(BF_4)_2$ (**2**) was obtained in 66% yield as yellow needles.

The identity of **2** was elucidated by X-ray crystallography, NMR spectroscopy, and IR spectroscopy. The solid-state structure observed for **2** is shown in Figure 1. It consists of two ruthenium atoms bridged by two chlorides (Ru−Ru distance of 3.8329(3) Å), with one N_2 molecule bound end-on to each metal center. The Ru1−N3 and Ru2−N4 distances are 1.950(2) Å and 1.944(2) Å, in good agreement with related monomeric complexes.[47,48]

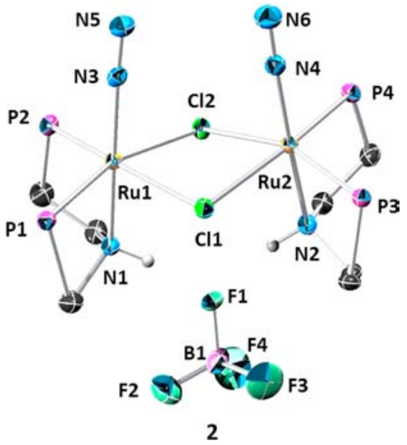

Figure 1. Thermal ellipsoid (50%) plot of the X-ray structure of **2**. Carbon atoms of the isopropyl groups, one BF_4 anion, solvent molecules and hydrogen atoms attached to carbon have been omitted for clarity.

The most interesting feature of **2** is that the dinitrogen molecules display a configuration where the two N_2 ligands are aligned in the same direction, with a small N3−Ru1−Ru2−N4 torsion angle of 4.3(1)°; in contrast, the Cl3−Ru1−Ru2−Cl4 torsion angle in **1** is almost 180°. The Ru metal centers in the $\{[HPNPRu(N_2)]_2(\mu\text{-}Cl)_2\}^{2+}$ moiety are related by a 2-fold axis and two mirror planes (C_{2v} symmetry). The N−N bond length of 1.103(3) Å, and a strong absorption band at 2161 cm^{-1} for the N−N stretch in the IR spectrum indicates a low degree of activation in the dinitrogen molecule. The geometry displayed by **2** is clearly enforced by formation of hydrogen bonds between the BF_4 anion and the amine N*H*. In the solid-state, H_{amine}-F distances found were 2.066(9) and 2.068(8) Å, considerably shorter than the sum of the van der Waals radii (2.67 Å). Further confirmation came from an electrospray ionization mass spectrometry (ESI-MS) experiment in acetonitrile, where the molecular ion corresponding to the protonated cation $\{[(HPNPRu)(\mu\text{-}Cl)_2(HPNPRu(N_2))](BF_4)\}^+$ (i.e., from loss of one N_2 ligand and one BF_4 anion bound) was detected at 1001 *m*/*z*.

The structure observed for **2** in the solid-state and by ESI-MS is retained in solution, as observed by NMR spectroscopy in $CDCl_3$. In the ^{31}P NMR spectrum only one sharp signal at 72.01 ppm is observed; more importantly, the ^{19}F NMR spectrum shows two signals very close to each other, at −151.41 and −151.47 ppm, indicative of tight ion pairing in

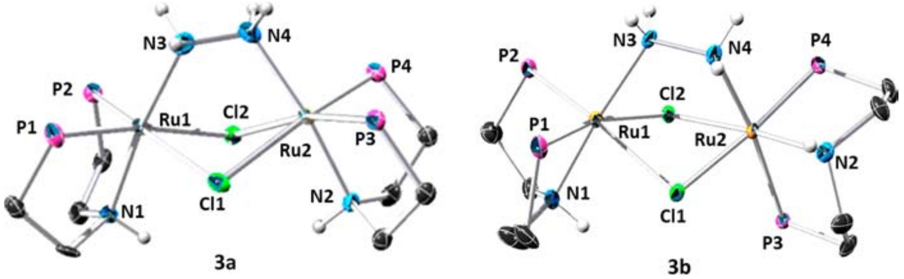

Figure 2. Thermal ellipsoid (50%) plot of the X-ray structures of **3a** and **3b**. Carbon atoms of the isopropyl groups, BF_4 anions, solvent molecules and hydrogen atoms attached to carbon have been omitted for clarity.

Table 1. Selected Bond Distances and Angles for Ru Complexes 2, 3a, 3b, 4, and 5

	2	3a	3b	4	5
Ru1−Ru2	3.8329(3) Å	3.5556(9) Å	3.525(1) Å	3.4121(4) Å	
Ru1−N3	1.950(2) Å	2.149(9) Å	2.125(7) Å	1.983(3) Å	2.159(2) Å[b]
Ru2−N4	1.944(2) Å	2.138(7) Å	2.246(7) Å	2.084(3) Å	
Ru1−Cl1	2.5025(6) Å	2.481(2) Å	2.480(2) Å	2.4510(9) Å	
Ru1−Cl2	2.5069(8) Å	2.495(2) Å	2.416(2) Å	2.454(1) Å	
N3−N4	3.411(8) Å (1.103(3) Å)[a]	1.435(9) Å	1.472(9) Å	1.289(5) Å	1.436(3) Å
N1−Ru1−N3	177.33(9)°	170.8(3)°	90.4(2)°	172.4(1)°	175.69(8)°
N2−Ru2−N4	178.1(1)°	171.8(3)°	174.7(3)°	168.7(1)°	70.9(1)°[c]
N3−Ru1−Ru2−N4	4.3(1)°	12.3(3)°	16.0(3)°	1.0(1)°	

[a] N3−N5 distance. [b] Ru-NH_3 distance. [c] $N_{hydazine}$−Ru1−$N_{hydrazine}$ angle.

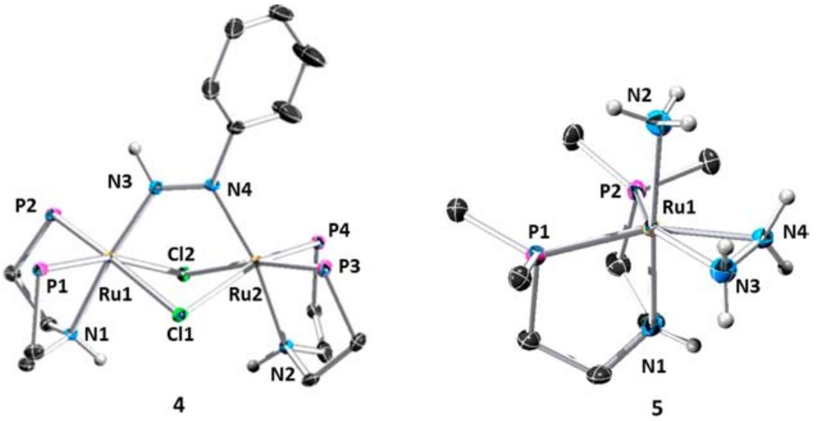

Figure 3. Thermal ellipsoid (50%) plot of the X-ray structures of **4** and **5**. Carbon atoms of the isopropyl groups, BF_4 anions, the Cl anion in **5**, solvent molecules and hydrogen atoms attached to carbon have been omitted for clarity.

this solvent. When the latter spectrum was recorded in THF, only a single peak was detected, consistent with fast exchange of the BF_4 counterions. This differing behavior in solution is consistent with the differences in dielectric constant of the solvents.

Reaction of **2** with 1 equiv of hydrazine in THF generates the complex $[(HPNPRu)_2(\mu^2\text{-}H_2NNH_2)(\mu\text{-}Cl)_2](BF_4)_2$ (**3**), obtained in 57% yield as yellow crystals after work up of the reaction mixture. Complex **3** crystallizes in two different conformations depending upon the solvent used. When a concentrated solution of **3** in chloroform is slowly evaporated, the solid-state structure shows a conformation (**3a**) similar to that observed for **2**, where the dinitrogen molecules have been displaced by the hydrazine ligand (Figure 2). **3a** shows a Ru−Ru distance of 3.5556(9) Å and Ru−$N_{hydrazine}$ distances of 2.149(9) and 2.138(7) Å (Table 1). The hydrazine ligand displays a zigzag conformation, with a N−N distance of 1.435(9) Å and a N3−Ru1−Ru2−N4 torsion angle of 12.3(3)°. This complex also shows close contacts between the N*H* protons of the HPNP ligand and a fluorine in the BF_4 anion (2.342(6) Å and 2.441(6) Å), and between the protons in the hydrazine and the BF_4 moieties (2.139(7) Å and 2.322(6) Å).

When **3** was crystallized from CH_2Cl_2/diethyl ether, the structure obtained showed a geometry where one HPNP ligand is rotated approximately 100° relative to the other about the Ru1−Ru2 axis (**3b**); no symmetry elements relate the two metal centers. In this conformation, one nitrogen in the hydrazine is trans to the nitrogen of the HPNP ligand on one Ru center and trans to a phosphorus in the other, making the Ru1−N3 distance approximately 0.10 Å shorter than Ru2−N4 (Figure 2). Relative to **3a**, the structure of **3b** shows a similar Ru1−Ru2 distance (3.525(1) Å) and a slightly elongated N−N bond in the hydrazine ligand (1.472(9) Å), that also displays a

Table 2. Selected Bond Distances and Angles for Ru Complexes 6, 7, 8, 9, and 10

	6^a	7^b	8^c	9^d	10^a
Ru1–Ru2	3.3020(4) Å	3.8078(5) Å		3.786(1) Å	3.324(1)
Ru1–X1	2.436(1) Å	1.62(10) Å	1.931(2) Å	2.200(2) Å	2.421(2) Å
Ru2–X2	2.543(1) Å	1.66(8) Å	1.962(2) Å	2.197(2) Å	2.556(2) Å
Ru1–Cl1	2.483(1) Å	2.496(1) Å	2.4350(5) Å	2.4772(9) Å	2.468(2) Å
Ru1–Cl2	2.525(1) Å	2.498(2) Å		2.516(1) Å	2.582(2) Å
N1–Ru1–X1	169.6(1)°	177(3)°	95.36(7)°	176.66(8)°	170.0(2)°
N2–Ru2–X2	91.0(1)°	171(2)°		176.30(8)°	88.7(2)°
X1–Ru1–Ru2–X2		4(3)°		1.17(8)°	

[a] X = Cl3. [b] X = H_2 centroid. [c] X = CO. [d] X = O.

zigzag conformation (the N3–Ru1–Ru2–N4 torsion angle being 16.0(3)°).

The ^1H NMR and ^{31}P NMR spectra show that **3a** is more stable in solution than **3b**. When a sample of pure **3b** was dissolved in CH_2Cl_2 and allowed to stand at 20 °C for 20 min, resonances due to both **3a** and **3b** were observed in the ^1H NMR spectrum. Six peaks in the region between 4.5 and 6.5 ppm are observed for **3b**, corresponding to the nonequivalent N–H protons (four from the hydrazine and two from the *H*PNP ligand). A singlet at 5.77 ppm in the same region was assigned to conformation **3a** (at −50 °C it splits into two broad singlets, integrating 2 to 1, corresponding to the hydrazine and HPNP protons). The ^{31}P NMR spectrum also shows two sets of signals, four doublets for the configuration in **3b**, and one singlet at 68.61 ppm for the one in **3a**. After 24 h, the ^1H NMR and ^{31}P NMR spectra show complete conversion to **3a**.

A mechanism involving reversible μ^2/μ^1 binding of the hydrazine (from bridging ligand to terminal) would account for the interconversion between **3a** and **3b**, and the presence of only one singlet for the hydrazine protons and the phosphorus atoms in the NMR spectra of **3a**. This postulate is supported by density functional theory (DFT) calculations: **3a** and the μ^1 bound species $Ru(NH_2NH_2)/Ru(N_2)$ (**3f**) have the same energy (within 0.4 kcal/mol), whereas **3b** is 4.5 kcal/mol less stable than **3a** (see Supporting Information).

Treatment of **2** with $PhHNNH_2$ generates two products: a yellow solid soluble in THF that could not be characterized, and a purple solid insoluble in THF. Crystallization of this purple solid from CH_2Cl_2/diethyl ether followed by an X-ray structure analysis showed the formation of $[(HPNPRu)_2(\mu^2\text{-}PhNNH)(\mu\text{-}Cl)_2](BF_4)_2$ (**4**), presumably, via the oxidation of phenylhydrazine to phenyldiazene (yield 13%). The solid-state structure displays a conformation similar to **2** and **3a** (Figure 3). As expected from the presence of an N–N double bond, the N–N, Ru–Ru, and Ru–N distances (1.289(5) Å, 3.4121(4) Å, 1.983(3) Å, and 2.084(3) Å, respectively) are shorter than those observed for **3a** and **3b**. The torsion angle N3–Ru1–Ru2–N4 is almost planar (1.0(1)°), instead of the zigzag conformation observed for the hydrazine adduct, and mirror symmetry is present in this plane. The ^1H NMR reveals a singlet at 15.55 ppm (1 H), for the N*H* proton in the phenyldiazene ligand. Disproportion of phenylhydrazine in this manner has precedent in related chemistry.[25,31,49]

We also explored the ability of complex **3** to produce ammonia from hydrazine. Treatment of **3** with HCl/H_2O, or HCl/Et_2O results in nearly complete conversion of the hydrazine ligand to ammonia characterized and quantified by the indophenol test[50] and ^1H NMR spectroscopy. No hydrazine was detected in these experiments. Catalytic disproportionation of hydrazine was also observed with **3**: when the complex was treated with excess of hydrazine (10 equiv) at room temperature, ammonia was produced in 26% yield based on hydrazine, with a production of almost six molecules of ammonia per dimer (Table 3). The same yield was obtained when $Cp_2Co/HLutBF_4$ was added to a mixture of **3** with 10 equiv of hydrazine, indicating that this combination is not effective in improving ammonia production under the experimental conditions tested.

Table 3. Ammonia Synthesis Results[a]

catalyst	mmol cmpd	Eq. N_2H_4	Eq. Cp_2Co	Eq. $HLutBF_4$	T.O.N.[b]	yield NH_3[c]
3	0.011	1.0	No	No	1.93	96%
3	0.010	12.3	No	No	5.90	26%
3	0.010	11.5	85	160	5.38	26%

[a] Reaction conditions: 10 mL THF, room temperature, 16 h. [b] Turn over number per Ru dimer molecule. [c] Yield calculated based on hydrazine. Ammonia was quantified by the indophenol test.[50] Average of at least three experiments.

To further explore the disproportionation process, we treated **3** with excess hydrazine. After work up of the product, an X-ray analysis showed the formation of the monometallic species $[HPNPRu(NH_3)(\kappa^2\text{-}N_2H_4)](BF_4)Cl$ (**5**) (Figure 3). The Ru–N bond distances for hydrazine, ammonia, and the HPNP ligand are very similar (2.157(2) Å, 2.159(2) Å, 2.149(3) Å, and 2.136(2) Å, respectively), and the N–N bond distance (1.436(3) Å) is essentially the same as in free hydrazine and in **3a**. The ^1H NMR spectrum is consistent with the proposed formula. The ammonia ligand appears as a singlet at 2.06 ppm and the hydrazine as a doublet at 6.38 ppm. Formation of **5** confirms the synthesis of ammonia by a disproportionation mechanism.

We also targeted the synthesis of a reduced ruthenium species in an effort to gain insights about possible reduction pathways. Complex **2** was treated with 2 equiv of Cp_2Co at room temperature in THF to give a yellow-orange suspension. After work up of the reaction mixture, $[(HPNPRu)_2(\mu\text{-}Cl)_3]BF_4$ (**6**) was obtained as an orange powder in 63% yield. The ^{31}P NMR spectrum contains two doublets at 77.1 ppm and 68.0 ppm, with an AX pattern and a J_{P-P} coupling of 32.4 Hz. X-ray diffraction analysis of **6** shows a pseudo 3-fold axis between the Ru atoms, with the HPNP ligands rotated by almost 120° with respect of each other around the Ru1–Ru2 axis (the N1–Ru1–Ru2–N2 torsion angle is 121.2(2)°, Figure 4).

When **2** was treated with H_2 (1 atm) for one week at 19 °C, both dinitrogen ligands were displaced by H_2; the bis-(dihydrogen) complex $\{[HPNPRu(H_2)]_2(\mu\text{-}Cl)_2\}(BF_4)_2$ (**7**) was subsequently isolated as yellow needles in 73% yield. A

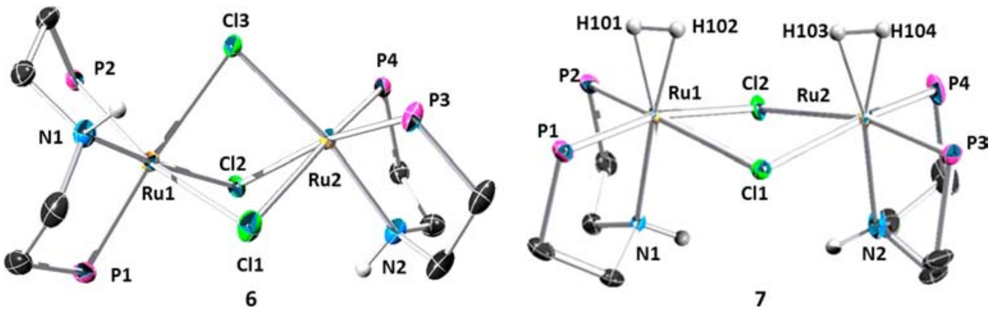

Figure 4. Thermal ellipsoid (50%) plot of the X-ray structures of **6** and **7**. Carbon atoms of the isopropyl groups, BF_4 anions, solvent molecules and hydrogen atoms attached to carbon have been omitted for clarity.

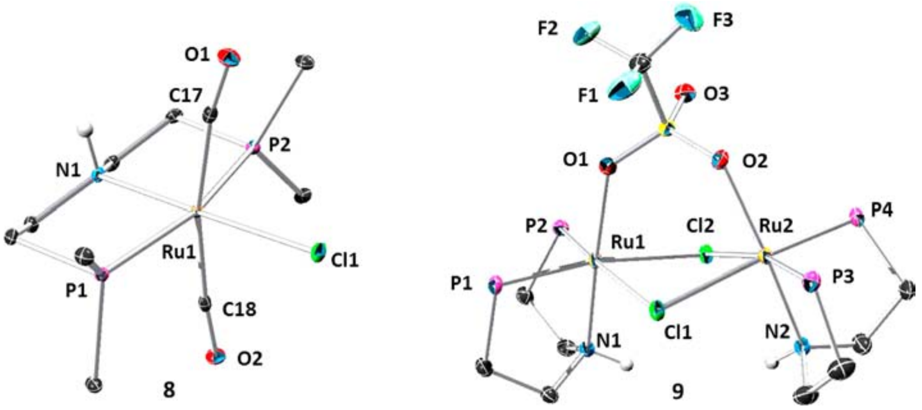

Figure 5. Thermal ellipsoid (50%) plot of the X-ray structures of **8** and **9**. Carbon atoms of the isopropyl groups, anions, solvent molecules and hydrogen atoms attached to carbon have been omitted for clarity.

broad singlet is observed in the ^1H NMR spectrum at −7.49 ppm, corresponding to the two bound H_2 molecules, whereas the ^{31}P NMR shows a singlet at 83.98 ppm. A T_1 experiment confirmed the presence of coordinated H_2 ligands ($T_1 = 27 \pm 2$ ms at 22 °C).

An X-ray analysis of **7** shows the geometry and metrical parameters to be close to those found in **2** (Figure 4). The dihydrogen atoms were found in the Fourier map and refined isotropically after fixing one Ru−H distance at 1.69 Å. When the reaction was performed with D_2 and HD, the corresponding complexes $\{[HPNPRu(D_2)]_2(\mu\text{-}Cl)_2\}(BF_4)_2$ (**7b**) and $\{[HPNPRu(HD)]_2(\mu\text{-}Cl)_2\}(BF_4)_2$ (**7c**) were produced. For **7c** the signal appears as a 1:1:1 triplet of triplets at −7.56 ppm in the ^1H NMR due to H−D coupling and P−H coupling. The $J_{\text{H-D}}$ coupling constant was 30.4 Hz, consistent with an H−H distance of 0.91 Å.[51]

The latter reaction is reversible: treatment of complex **7** with excess N_2 regenerates **2** over several days. Following the reaction using ^1H NMR and ^{31}P NMR spectroscopy (see the Supporting Information) shows that the two reactions proceed through the same intermediate, assigned as the mixed species $\{[HPNPRu(H_2)](\mu\text{-}Cl)_2[HPNPRu(N_2)]\}(BF_4)_2$ (**2b**). The latter shows a broad singlet at −7.41 ppm in the ^1H NMR spectrum for the H_2, and two singlets in the ^{31}P NMR spectrum, at 84.69 ppm and 71.95 ppm, due to the two different Ru centers. The reversible binding of H_2 was investigated by DFT calculations, which showed that the dinitrogen complex **2** has a lower energy than the mixed dihydrogen/dinitrogen complex (**2b**) and the bis dihydrogen complex (**7**) by 4.5 and 10.2 kcal/mol respectively (see Supporting Information).

Complex **2** reacts with CO (1 atm) in CH_2Cl_2 to form the monomeric complex $[HPNPRu(CO)_2Cl]BF_4$ (**8**) as colorless, block like crystals, obtained in 31% yield. The X-ray structure (Figure 5) shows the CO ligands trans to each other with C−O distances of 1.135(2) Å and 1.136(2) Å, while the IR spectrum shows the carbonyl stretch at 2008 cm^{-1}.

Reaction of **1** with $AgOSO_2CF_3$ produces the complex $[(HPNPRu)_2(\mu^2\text{-}OSO_2CF_3)(\mu\text{-}Cl)_2]OSO_2CF_3$ (**9**) as orange, block-like crystals in 84% yield. The ^1H NMR, ^{31}P NMR, and ^{19}F NMR spectra for **9** are consistent with one triflate anion coordinating to the metal centers in solution. The ^{31}P NMR spectrum shows two doublets at 70.83 and 70.43 ppm, with an AB pattern and a $J_{\text{P−P}}$ coupling of 32.4 Hz. The ^{19}F NMR shows two singlets in a 1:1 ratio, one at −77.26 ppm and the other at −77.67 ppm, in agreement with one bound and one unbound triflate ligand.

Crystals suitable for an X-ray diffraction study of **9** were grown from a concentrated solution in CH_2Cl_2 layered with diethyl ether. Selected bond lengths and angles are shown in Table 2 and an ORTEP diagram is provided in Figure 5. Complex **9** has the same bimetallic $RuCl_2Ru$ core as **2** (Ru1−Ru2 distance 3.786(1) Å), with one triflate coordinated to the two metal centers via two oxygen atoms. The distances and angles around the metal centers are consistent with those found **2**, and the Ru1−O1 and Ru2−O2 distances (2.200(2) Å and 2.197(2) Å respectively) are in good agreement with related molecules.[52,53] As for **2**, **3a**, **4**, and **7**, in complex **9** the HPNP ligands are placed at 0° to each other around the Ru1−Ru2 axis, in this case due to the presence of the triflate ligand (the O1−Ru1−Ru2−O2 torsion angle is 1.17(8)°).

Table 4. Crystal Data and Structure Refinement for Structures 2−10

	2	**3a**	**3b**	**4**	**5**
formula	$C_{32}H_{74}B_2Cl_2F_8N_6P_4Ru_2\cdot CH_2Cl_2$	$C_{32}H_{78}B_2Cl_2F_8N_4P_4Ru_2\cdot 4CHCl_3$	$C_{32}H_{78}B_2Cl_2F_8N_4P_4Ru_2$	$C_{38}H_{80}B_2Cl_2F_8N_4P_4Ru_2$	$C_{16}H_{45}BClF_4N_4P_2Ru\cdot CH_2Cl_2$
FW (g/mol)	1198.44	1567.00	1089.52	1163.60	662.75
T (K)	113(2)	100(2)	100(2)	100(2)	100(2)
space group	$P2_1/c$	$P\bar{1}$	$Pbca$	Cc	$P2_12_12_1$
a (Å)	15.7122(5)	11.8002(4)	13.171(5)	10.1804(6)	9.2003(2)
b (Å)	14.9191(5)	13.2180(4)	18.485(5)	27.0385(18)	15.0373(4)
c (Å)	22.5318(8)	22.3853(7)	40.465(5)	19.0234(11)	20.8396(5)
α (deg)	90	83.049(2)	90	90	90
β (deg)	104.3220(10)	80.921(2)	90	93.132(3)	90
γ (deg)	90	67.533(2)	90	90	90
V (Å^3)	5117.6(3)	3179.06(18)	9852(5)	4953.8(5)	2883.11(12)
Z	4	2	8	4	4
λ (Å)	0.71073	0.71073	0.71073	0.71073	0.71073
μ (mm^{-1})	0.985	1.219	0.909	0.910	0.972
# unique reflections	9460	11647	9153	4623	5317
R_{int}	0.0249	0.0674	0.0874	0.0281	0.0300
R [$I > 2\sigma(I)$]	0.0267	0.0625	0.0760	0.0285	0.0199
$R(F_o)$	0.0347	0.1079	0.0980	0.0310	0.0200
$R_w(F_o)$	0.0853	0.1725	0.1707	0.0706	0.0466
GOF	1.131	1.061	1.192	1.054	1.204
	6	**7**	**8**	**9**	**10**
formula	$C_{32}H_{74}BCl_3F_4\ N_2P_4Ru_2$	$C_{32}H_{78}B_2Cl_2F_8N_2P_4Ru_2\cdot CH_2Cl_2$	$C_{18}H_{37}BCl\ F_4NO_2P_2Ru$	$C_{34}H_{74}Cl_2\ F_6N_2O_6P_4Ru_2S_2$	$C_{56}H_{94}BCl_3N_2P_4Ru_2$
FW (g/mol)	1006.11	1146.43	584.77	1181.99	1238.51
T (K)	100(2)	100(2)	100(2)	144(2)	109(2)
space group	$P\bar{4}2_1c$	$P2_12_12_1$	$P2_12_12_1$	$P2_1/n$	$P2_1/c$
a (Å)	25.3447(9)	16.2143(6)	11.7009(5)	10.242(2)	15.8722(14)
b (Å)	25.3447(9)	16.7728(7)	12.2407(5)	34.018(8)	19.2210(17)
c (Å)	14.4707(6)	18.0133(7)	17.5457(7)	14.882(3)	19.4031(17)
α (deg)	90	90	90	90	90
β (deg)	90	90	90	103.049(4)	95.7470(10)
γ (deg)	90	90	90	90	90
V (Å^3)	9295.3(8)	4898.9(3)	2513.02(18)	5051.0(2)	5889.7(9)
Z	8	4	4	4	4
λ (Å)	0.71073	0.71073	0.71073	0.71073	0.71073
μ (mm^{-1})	1.003	1.023	0.902	0.976	0.795
# unique reflections	8224	8983	4550	9286	10916
R_{int}	0.0432	0.0318	0.0250	0.0500	0.0458
R [$I > 2\sigma(I)$]	0.0336	0.0405	0.0164	0.0318	0.0816
$R(F_o)$	0.0398	0.0437	0.0175	0.0410	0.0962
$R_w(F_o)$	0.1069	0.1058	0.0377	0.0795	0.1852
GOF	1.235	1.103	1.080	1.037	1.376

An analogous reaction was performed with 2 equiv of $AgBPh_4$ instead of $AgOSO_2CF_3$, and $[(HPNPRu)_2(\mu\text{-}Cl)_3]$-$BPh_4$ (**10**) was isolated as orange, block like crystals, in 68% yield. The NMR spectra as well as the X-ray structure show almost identical parameters as those observed for **6**. Attempts to abstract the second chloride (e.g., by heating **10** to reflux in THF for 48 h with excess of $AgBPh_4$) were unsuccessful and **10** was recovered as the major product.

■ CONCLUSIONS

The HPNP ligand is a good supporting scaffold to study the chemistry of bimetallic ruthenium complexes. A series of complexes with N_2, H_2, N_2/H_2, bridging diazene, and hydrazine ligands were synthesized and characterized. The system facilitates the study of interconversion reactions related to those proposed as steps in the reduction of nitrogen to ammonia by the nitrogenase enzyme. Hydrazine was found to displace both dinitrogen ligands on adjacent Ru atoms in complex **2** to form a new species **3** with hydrazine bridging the two metal centers. This complex further reacts with hydrazine to produce the monomeric species **5** with ammonia and hydrazine bound to the metal center. The reaction of **2** with phenylhydrazine generates the diazene species **4**. Complex **3** promotes the formation of ammonia from hydrazine stoichiometrically (by reaction with protons) or catalytically by disproportionation.

■ EXPERIMENTAL SECTION

General Considerations. Unless otherwise noted, all reactions were performed using standard Schlenk techniques under N_2-atm or in a N_2-atm glovebox. Solvents were dried by passing through a column of activated alumina and degassed with nitrogen.[54] $CDCl_3$ and CD_2Cl_2 were dried over CaH_2 and vacuum transferred. All NMR spectra were obtained in $CDCl_3$ or CD_2Cl_2 at ambient temperature using Bruker AVQ-400, AV-500, DRX-500 or AV-600 spectrometers. ^{1}H NMR chemical shifts (δ) were calibrated relative to residual solvent peak. The assignments were confirmed by ^{1}H−^{1}H COSY, ^{1}H−^{13}C HSQC, and ^{13}C-DEPT135 NMR spectroscopy. Melting points were determined using sealed capillaries prepared under a nitrogen atmosphere. Infrared (IR) spectra were recorded with a Thermo Scientific Nicolet iS10 series FTIR spectrophotometer as a powder or Nujol mull between KBr plates, or in solution with a CaF_2 cell. Elemental analyses were performed at the University of California, Berkeley Microanalytical Facility. Single crystal X-ray diffraction analyses (Table 4) were performed at the University of California, Berkeley CHEXRAY facility. The remaining starting materials were obtained from Aldrich and used without further purification.

$(HPNPRuCl)_2(\mu\text{-}Cl)_2$ (1). A solution of HPNP (1.3 g, 4.3 mmol, HPNP = $(^iPr_2PCH_2CH_2)_2NH$) in 20 mL of ethanol was added to a suspension of $[(COD)RuCl]_2(\mu\text{-}Cl)_2$ (1.2 g, 2.1 mmol) in 80 mL of ethanol. The reaction mixture was heated at reflux for 16 h, and the solution color turned from brown to orange. The solvent was removed under vacuum, and the solid residue was extracted with CH_2Cl_2. Concentration of the solution and precipitation with hexane gave an orange powder (1.6 g, 80%). ^{1}H NMR, ^{31}P NMR spectra matched reported literature values.[46]

$\{[HPNPRu(N_2)]_2(\mu\text{-}Cl)_2\}(BF_4)_2$ (2). A solution of $AgBF_4$ (0.58 g, 3.0 mmol) in 20 mL of THF was added dropwise to a suspension of **1** (1.4 g, 1.5 mmol) in 30 mL of THF at room temperature and nitrogen atm. A white precipitate immediately appeared, and the solution color changed from orange to yellow. The reaction mixture was stirred overnight. The solvent was removed under vacuum, and the product extracted with CH_2Cl_2 (3 × 20 mL) and filtered through Celite. The solution was concentrated and layered with hexane to give yellow, needle-like crystals (1.1 g, 66%). Crystals suitable for an X-ray diffraction study were grown from a concentrated solution of CH_2Cl_2 layered with diethyl ether. ^{1}H NMR ($CDCl_3$) 5.76 (s (br), 2H, NH), 3.21 (m, 4H, NCH_2), 2.94 (m, 4H, NCH_2), 2.58 (m, 4H, $PCH(CH_3)_2$), 2.14 (m, 8H, $PCH(CH_3)_2$ (4) and PCH_2 (4)), 1.96 (m, 4H, PCH_2), 1.49−1.26 (m, 48H, $PCH(CH_3)_2$) ^{31}P NMR 72.01 (s, 4P). ^{19}F NMR −151.41 (s), −151.47 (s). ^{13}C NMR 51.3 (s, NCH_2), 30.1 (t, $PCH(CH_3)_2$), 25.9 (dt, CH_2P), 25.0 (dt, $PCH(CH_3)_2$), 20.5−18.6 (m, CH_3). IR (cm^{-1}, Nujol mull) 3257 (m), 2161 (s, N_2), 1283 (w), 1259 (m), 1244 (m), 1061 (s), 959 (m), 929 (w), 906 (m), 827 (m), 818 (w), 791 (w), 729 (m), 698 (m), 665 (w), 607 (w), 520 (w). Anal. Calc: C, 34.52; H, 6.70; N, 7.55. Observed C, 34.49; H, 6.62; N, 7.32. Mp 140−143 °C (d).

$[(HPNPRu)_2(\mu^2\text{-}H_2NNH_2)(\mu\text{-}Cl)_2](BF_4)_2$ (3). Dry hydrazine (9 μL, 0.29 mmol) was added via syringe to a suspension of **2** (0.32 g, 0.29 mmol) in 25 mL of THF at room temperature and stirred overnight. The reaction goes from yellow suspension to a yellow-orange suspension. The solution was filtered over Celite, and the remaining solid washed with THF (2 × 5 mL). The solution was evaporated to dryness, and the yellow solid formed was redissolved in CH_2Cl_2. After filtration, the solution was concentrated and layered with diethyl ether, to yield rod-like, yellow crystals (0.18 g, 57%). (**3a**) Crystals suitable for an X-ray diffraction study were grown from a concentrated solution of $CHCl_3$ slowly evaporated; (**3b**) crystals suitable for an X-ray diffraction study were grown from a concentrated solution of CH_2Cl_2 layered with diethyl ether. **3a** ^{1}H NMR (CD_2Cl_2) 5.77 (s, 6H, NH_2 and NH), 3.00 (m, 8H, NCH_2 (4) and PCH_2 (4)), 2.50 (m, 4H, NCH_2), 2.19 (m, 4H, $PCH(CH_3)_2$), 1.86 (m, 4H, PCH_2), 1.48 (m, 4H, $PCH(CH_3)_2$), 1.41−1.20 (m, 48 H, $PCH(CH_3)_2$). ^{31}P NMR 68.61 (s). ^{19}F NMR −151.21 (s). ^{13}C NMR 51.43 (NCH_2), 30.01 (t, $PCH(CH_3)_2$), 28.13 (m, PCH_2), 25.30 (t, $PCH(CH_3)_2$), 20.20 (s, CH_3), 20.06 (s, CH_3), 19.87 (s, CH_3), 18.64 (s, CH_3). **3b** ^{1}H NMR (CD_2Cl_2) 6.49 (d, 1H, NH_2), 5.90 (t, 1H, NH_2), 5.62 (d, 1H, NH_2), 5.46 (t, 1H, NH_2), 4.94 (s, 1H, NH), 4.75 (s, 1H, NH). ^{31}P NMR 75.11 (d), 68.58 (d), 75.52 (d), 62.99 (d). The rest of the peaks for **3b** could not be assigned due transformation to **3a** and overlap. IR (cm^{-1}, Nujol mull) 3331 (m, NH_2), 3273 (m NH_2)), 1598 (m, NH_2)), 1051 (s), 1335 (w), 1256 (w), 1051 (s), 998 (s), 882 (s), 826 (s), 763 (m), 700 (m). Anal. Calc: C, 35.28; H, 7.22; N, 5.14. Observed C, 35.02; H, 7.02; N, 5.02. Mp 185−188 °C (d).

$[(HPNPRu)_2(\mu^2\text{-}HNNPh)(\mu\text{-}Cl)_2](BF_4)_2$ (4). Dry PhHNNH$_2$ (27 μL, 0.27 mmol) was added via syringe to a suspension of **2** (0.30 g, 0.27 mmol) in 25 mL of THF at room temperature and stirred overnight. The color of the suspension changed from yellow to purple. The solution was filtered, and the remaining purple solid washed with THF (2 × 5 mL). The solid was dissolved in CH_2Cl_2 and filtered over Celite. The solution was concentrated and layered with diethyl ether, to yield plate-like, dark red crystals (0.04 g, 13%). Crystals suitable for an X-ray diffraction study were grown from a concentrated solution of CH_2Cl_2 layered with diethyl ether. ^{1}H NMR (CD_2Cl_2) 15.55 (s, 1H, PhNN*H*), 7.71 (d, 2H, *o*-C_6H_5), 7.63 (7, 1H, *p*-C_6H_5), 7.55 (t, 2H, *m*-C_6H_5), 6.31 (m, 1H, NH), 6.27 (m, H, NH), 3.26 (m, 4H, NH_2), 2.88 (m, 2H, NH_2), 2.69 (m, 2H, NH_2), 2.58 (m, 2H, $PCH(CH_3)_2$), 2.47 (m, 2H, $PCH(CH_3)_2$), 2.25 (m, 8H, $PCH(CH_3)_2$ (4) and PCH_2 (4)), 2.05 (m, 2H, PCH_2), 1.98 (m, 2H, PCH_2), 1.50−0.88 (m, 48 H, $PCH(CH_3)_2$). ^{31}P NMR 63.60 (s), 56.55 (s). ^{19}F NMR −152.01 (s). ^{13}C NMR 156.56 (*i*-C), 130.02 (*m*-C), 128.53 (*p*-C), 121.63 (*m*-C), 50.30 and 50.03 (s, NCH_2), 37.34 (m, $PCH(CH_3)_2$), 31.51 and 29.26 (m, CH_2P), 26.87 and 24.92 (m, $PCH(CH_3)_2$), 21.25−19.02 (m, CH_3). IR (cm^{-1}, Nujol mull) 3259 (w, NH), 3160 (w, NH)), 1260 (s, N=N)), 1021 (s),800 (m), 720 (w), 689 (w). Anal. Calc: C, 39.22; H, 6.93; N, 4.81. Observed C, 38.86; H, 6.82; N, 4.67. Mp 245−249 °C (d).

$[HPNPRu(NH_3)(\kappa^2\text{-}N_2H_4)](BF_4)Cl$ (5). Dry hydrazine (36 μL, 1.1 mmol) was added via syringe to a solution of **3** (0.05 g, 0.05 mmol) in 5 mL of CH_2Cl_2 at room temperature under argon atmosphere. The solution color changed from yellow to light yellow. After 48 h the solution was layered with diethyl ether to yield rod-like, colorless crystals (0.03 g, 52%). Crystals suitable for an X-ray diffraction study were grown from a concentrated solution of CH_2Cl_2 layered with diethyl ether. ^{1}H NMR (CD_2Cl_2) 6.38 (d, 4 H, N_2H_4), 5.93 (s, 1H, NH), 2.77 (m, 2H, $PCH(CH_3)_2$), 2.65 (m, 2H, NH_2), 2.58 (m, 2H, NH_2), 2.47 (m, 2H, PCH_2), 2.15 (m, 2H, PCH_2), 2.06 (s, 3H, NH_3), 1.91 (m, 2H, $PCH(CH_3)_2$), 1.39−1.11 (m, 24H, $PCH(CH_3)_2$). ^{31}P NMR 80.19 (s). ^{19}F NMR −149.24 (s), 149.29 (s). IR (cm^{-1}, Nujol mull) 3287 (m, NH), 3110 (m, NH_2)), 1614 (m), 1574 (m), 1427 (m), 1300 (m), 1251 (w), 1150 (m), 1030 (s), 1003 (s), 926 (m), 880 (s), 818 (s), 727 (s), 698 (s). **5** CH_2Cl_2 Anal. Calc: C, 30.78; H, 7.00; N, 8.45. Observed C, 30.69; H, 7.14; N, 8.84. Mp 97−100 °C (d).

$[(HPNPRu)_2(\mu\text{-}Cl)_3]BF_4$ (6). A solution of cobaltocene (0.11 g, 0.58 mmol) in 10 mL of THF was added dropwise to a suspension of **2** (0.30 g, 0.27 mmol) in 15 mL of THF at room temperature. The color of the suspension changed from a yellow to yellow-orange. The reaction mixture was stirred overnight. The solvent was removed under vacuum, and the product washed with diethyl ether (2 × 5 mL) and THF (3 × 5 mL). The analytically pure product was obtained as an orange powder (0.17 g, 63%). Crystals suitable for an X-ray diffraction study were grown from a concentrated solution of CH_2Cl_2 layered with diethyl ether. ^{1}H NMR 4.30 (s (br), 2H, NH), 3.15 (m, 2H, $PCH(CH_3)_2$), 2.86 (m, 4H, NCH_2), 2.75 (m, 2H, $PCH(CH_3)_2$), 2.07 (m, 4H, NCH_2), 2.04 (m, 2H, $PCH(CH_3)_2$), 1.91 (m, 4H, PCH_2), 1.72 (m, 2H, $PCH(CH_3)_2$), 1.51−1.08 (m, 52H, $PCH(CH_3)_2$ (48) and PCH_2 (4)) ^{31}P NMR 77.14 (d, 2P), 68.0 (d, 2P). ^{19}F NMR −152.29 (s), −152.34 (s). ^{13}C NMR 53.5 (s, NCH_2), 51.8 (s, NCH_2), 31.2 (d, $PCH(CH_3)_2$), 29.6 (d, CH_2P), 29.3 (t, $PCH(CH_3)_2$), 26.4 (d, CH_2P), 26.4 (d, $PCH(CH_3)_2$), 20.9−18.8 (m, CH_3). IR (cm^{-1}, Nujol mull) 3118 (m), 1377 (m), 1325 (w), 1260 (m), 1040 (s), 687 (m), 834 (m), 801 (s), 494 (w). Anal. Calc: C, 38.20; H, 7.41; N, 2.78. Observed C, 38.50; H, 7.24; N, 2.63. Mp 282−284 °C.

$\{[HPNPRu(H_2)]_2(\mu\text{-}Cl)_2\}(BF_4)_2$ (7). A solution of **2** (0.30 g, 0.27 mmol) in 20 mL of CH_2Cl_2 was evacuated, and the atmosphere was replaced with H_2 (1 atm), and stirred for 7 days. No change of color is observed. The solution was concentrated and layered with hexane under H_2 atmosphere, to yield yellow, needle-like crystals (0.21 g, 73%). Crystals suitable for an X-ray diffraction study were grown from a concentrated solution of CH_2Cl_2 layered with diethyl ether under H_2 atmosphere. ^{1}H NMR ($CDCl_3$) 6.33 (s (br), 2H, NH), 3.50 (m, 4H, NCH_2), 3.01 and 2.89 (m, 4H, NCH_2), 2.33 (m, 4H, $PCH(CH_3)_2$), 2.18 (m, 4H, PC*H*(CH$_3$)$_2$), 1.96 (m, 4H, PC*H*$_2$), 1.86 (m, 4H, PC*H*$_2$), 1.51−1.05 (m, 48H, PCH(C*H*$_3$)$_2$), −7.49 (s (br), 4H, *H*$_2$). ^{31}P NMR 83.98 (s). ^{19}F NMR −151.71 (s), −151.75 (s). ^{13}C NMR 50.4 (s, NCH$_2$), 29.1 (m, PCH(CH$_3$)$_2$), 25.9 (m, CH$_2$P), 23.9 (m, PCH(CH$_3$)$_2$), 21.0−18.0 (m, CH$_3$). IR (cm^{-1}, Nujol mull) 3259 (w), 1260 (m), 1259 (m), 1056 (s), 1061 (s), 800 (m), 668 (w). Anal. Calc: C, 36.21; H, 7.41; N, 2.64. Observed C, 35.74; H, 7.34; N, 2.61 (N$_2$ readily displaces H$_2$). Mp 161−164 °C (d).

{[HPNPRu(D$_2$)]$_2$(μ-Cl)$_2$}(BF$_4$)$_2$ (7b). A solution of **2** (30 mg, 0.027 mmol) in 0.5 mL of CDCl$_3$ was placed in a J. Young NMR tube. The solution was cooled using liquid nitrogen, evacuated, the atmosphere replaced with D$_2$, and the solution was warmed to room temperature (this procedure was repeated 3 times). The reaction was monitored by ^{31}P NMR spectroscopy, and after 4 days the reaction was more than 90% complete. The presence of the mixed species {[HPNPRu(D$_2$)](μ-Cl)$_2$[HPNPRu(N$_2$)]}(BF$_4$)$_2$ was still observed. ^{2}H NMR (CDCl$_3$) −7.55 (s). ^{31}P NMR 83.94 (s).

{[HPNPRu(HD)]$_2$(μ-Cl)$_2$}(BF$_4$)$_2$ (7c). The reaction was carried out analogous to that of **7b** with HD. ^{1}H NMR (CDCl$_3$) −7.56 (tt, HD), $J_{\text{H-D}}$ 30.4 Hz, $J_{\text{H−P}}$ 5.6 Hz. ^{31}P NMR{^{1}H} 83.95 (s).

[HPNPRu(CO)$_2$Cl]BF$_4$ (8). A solution of **2** (0.25 g, 0.22 mmol) in 15 mL of CH$_2$Cl$_2$ was evacuated, and the atmosphere was replaced with CO (1 atm), and stirred overnight. The solution color changed from yellow to pale yellow (almost colorless). The solution was concentrated and layered with diethyl ether, to yield block-like, colorless crystals (0.08 g, 31%). Crystals suitable for an X-ray diffraction study were grown from a concentrated solution of CH$_2$Cl$_2$ layered with diethyl ether. ^{1}H NMR 4.70 (s (br), 1H, N*H*), 3.36 (m, 2H, PC*H*$_2$), 2.66 (m, 4H, PC*H*(CH$_3$)$_2$), 2.28 (m, 2H, PC*H*$_2$), 2.03 (m, 4H, NC*H*$_2$), 1.61−1.32 (m, 24H, PCH(C*H*$_3$)$_2$). ^{31}P NMR 49.79 (s). ^{19}F NMR −150.08 (s), −150.13 (s). ^{13}C NMR 199.8 (s, CO), 194.2 (s,CO), 57.7 (s, NCH$_2$), 31.8 (t, PCH(CH$_3$)$_2$), 27.4 (t, CH$_2$P), 26.6 (t, PCH(CH$_3$)$_2$), 19.9 (s, CH$_3$), 19.2 (s, CH$_3$), 19.2 (s, CH$_3$), 19.0 (s, CH$_3$). IR (cm^{-1}, Nujol mull) 3264 (m), 2090 (m), 2008 (s, CO), 1991 (s, CO), 1377 (m), 1104 (s), 1059 (s), 834 (m), 788 (w), 707 (w), 669 (w), 585 (s). Anal. Calc: C, 36.97; H, 6.33; N, 2.40. Observed C, 36.71; H, 6.33; N, 2.33. Mp 301−304 °C (d).

[(HPNPRu)$_2$(μ^2-OSO$_2$CF$_3$)(μ-Cl)$_2$]OSO$_2$CF$_3$ (9). A solution of AgOSO$_2$CF$_3$ (0.16 g, 0.62 mmol) in 10 mL of THF was added dropwise to a suspension of (HPNPRuCl)$_2$(μ-Cl)$_2$ (0.30 g, 0.31 mmol) in 15 mL of THF at room temperature. A white precipitate appeared, and the color of the solution changed from orange to yellow. The reaction mixture was stirred overnight. The solvent was removed under vacuum, the product was extracted with CH$_2$Cl$_2$ (3 × 20 mL) and filtered through Celite. The solution was concentrated and layered with hexane to give orange, block-like crystals (0.31 g, 84%). Crystals suitable for an X-ray diffraction study were grown from a concentrated solution of CH$_2$Cl$_2$ layered with diethyl ether. ^{1}H NMR 5.94 (s (br), 2H, N*H*), 3.26 (m, 2H, PC*H*(CH$_3$)$_2$), 2.95 (m, 4H, PC*H*(CH$_3$)$_2$ (2), NC*H*$_2$ (2)), 2.73 (m, 2H, NC*H*$_2$), 2.45 (m, 2H, NC*H*$_2$), 2.33 (m, 2H, NC*H*$_2$), 2.11 (m, 2H, PC*H*(CH$_3$)$_2$), 2.00 (m, 4H, PC*H*$_2$), 1.93 (m, 2H, PC*H*(CH$_3$)$_2$), 1.6−1.2 (m, 48, PCH(C*H*$_3$)$_2$), 1.10 (m, 4H, PC*H*$_2$). ^{31}P NMR 70.83 (d, 2P), 70.43 (d, 2P). ^{19}F-NMR −77.26 (s, 3F), −77.67 (s, 3F). ^{13}C NMR 54.8 (d, NCH$_2$), 31.1 (d, PCH(CH$_3$)$_2$), 30.2 (d, PCH(CH$_3$)$_2$), 29.5 (d, PCH$_2$), 27.3 (d, PCH$_2$), 25.0 (m, PCH(CH$_3$)$_2$), 19.7−19.1(m, CH$_3$). IR (cm^{-1}, Nujol mull) 3444 (w), 1295 (s), 1243 (s) 1224 (s), 1159 (s), 1029 (s), 880 (w), 828 (w), 723 (m), 637 (w), 574 (w), 517 (w). Anal. Calc: C, 34.55; H, 6.31; N, 2.37; S, 5.43. Observed C, 34.67; H, 6.24; N, 2.52; S, 5.83. M*p* > 300 °C.

[(HPNPRu)$_2$(μ-Cl)$_3$]BPh$_4$ (10). A solution of AgBPh$_4$ (0.34 g, 0.80 mmol) in 10 mL of THF was added dropwise to a suspension of (HPNPRuCl)$_2$(μ-Cl)$_2$ (0.30 g, 0.31 mmol) in 15 mL of THF at room temperature. A white precipitate appears, and the solution color changed from orange to yellow-orange. The reaction mixture was stirred overnight, and then heated to reflux for 24 h. The solvent was removed under vacuum, the product was extracted with CH$_2$Cl$_2$ (3 × 20 mL), and filtered through Celite. The solution was concentrated and layered with diethyl ether to yield orange, block-like crystals (0.26 g, 68%). Crystals suitable for an X-ray diffraction study were grown from a concentrated solution of CH$_2$Cl$_2$ layered with diethyl ether. ^{1}H NMR 7.44 (m (br), 8H, *m-H*, BPh$_4$), 7.03 (t, 8H, *o-H*, BPh$_4$), 6.88 (t, 4H, *p-H*, BPh$_4$), 3.96 (s (br), 2H, N*H*), 3.10 (m, 2H, PC*H*(CH$_3$)$_2$), 2.82 (m, 2H, PC*H*(CH$_3$)$_2$), 2.54 (m, 2H, NC*H*$_2$), 2.15 (m, 2H, NC*H*$_2$), 2.09 (m, 2H, NC*H*$_2$), 1.83 (m, 6H, NC*H*$_2$ (2), PC*H*$_2$ (4)), 1.72 (m, 2H, PC*H*(CH$_3$)$_2$), 1.55−1.14 (m, 52H, PC*H*(CH$_3$)$_2$ (2), PC*H*$_2$ (2), PCH(C*H*$_3$)$_2$ (48)), 0.89 (m, 2H, PC*H*$_2$). ^{31}P NMR 76.75 (d, 2P), 67.92 (d, 2P). ^{13}C NMR 136.6 (*i-C*, BPh$_4$), 125.9 (*o-C*, *m-C*, BPh$_4$), 122.0 (*p-C*, BPh$_4$), 51.9 (d, NCH$_2$), 31.3 (d, PCH(CH$_3$)$_2$), 29.5 (d, PCH$_2$), 29.2 (t, PCH(CH3)2), 20.7−18.8 (m, CH$_3$). IR (cm^{-1}, powder) 3249 (w), 3053 (w), 2954 (m), 2928 (m), 2869 (m), 1580 (w), 1458 (s), 1427 (m), 1404 (w), 1388 (m), 1368 (m), 1252 (w), 1183 (w), 1087 (s), 1053 (m), 1031 (m), 883 (s), 816 (s). Anal. Calc: C, 54.30; H, 7.65; N, 2.26. Observed C, 54.57; H, 7.73; N, 2.38. Mp 285−288 °C.

Ammonia Synthesis by Disproportionation of Hydrazine.[20] In a typical experiment, 3 μL of hydrazine (0.10 mmol) was added to a suspension of **3** (11.0 mg, 0.010 mmol) in 10 mL of THF. The reaction mixture was stirred for 16 h, and 0.2 mL of concentrated HCl were added via syringe. The volatiles were removed under vacuum, and 4 M aqueous NaOH (15 mL) was added under argon. Between 10−12 mL of the solution were distilled on 12 mL of H$_2$SO$_4$ (0.5 M), and the volume was increased to 25 mL with distilled water. The amount of ammonia produced was analyzed by the indophenol test.[50] Additionally, the reaction mixture was treated with HCl/Et$_2$O (1M), and the formation of ammonia confirmed by ^{1}H NMR in *d*^{6}-DMSO.

Ammonia Synthesis by Reaction of 4 with Hydrazine, Cobaltocene, and Lutidinium Tetrafluoroborate.[27] In a typical experiment **4** (11.0 mg, 0.010 mmol)), cobaltocene (160 mg, 0.85 mmol) and lutidinium (320 mg, 1.6 mmol) were placed in a Schlenk tube. THF (10 mL) and 3 μL of hydrazine (0.10 mmol) were added via syringe at −78 °C. The reaction mixture was warmed to room temperature, stirred for 16 h, and worked up as for the disproportionation reaction.

Ammonia Synthesis by Reaction with HCl. The above procedure was followed without the addition of hydrazine. The formation of ammonia was quantified by the indophenol test and confirmed by ^{1}H NMR. Hydrazine presence was assessed by the *p*-(dimethylamino) benzaldehyde test.[55]

Crystallographic Analyses. Single crystals of **2** to **10** were coated in Paratone-N oil, mounted on a Kapton loop, and transferred to a Bruker SMART APEX or APEX II QUAZAR diffractometer with CCD area detector,[56] centered in the beam, and the crystal was cooled during data collection by a nitrogen flow low-temperature apparatus previously calibrated by a thermocouple placed at the same position as the crystal. Preliminary orientation matrices and cell constants were determined by collection of 60 30-s frames, followed by spot integration and least-squares refinement. A data collection strategy was computed with COSMO to ensure a redundant and complete data set, and the raw data were integrated using SAINT.[57] The data were corrected for Lorentz and polarization effects, but no correction for crystal decay was applied. An empirical absorption correction based on comparison of redundant and equivalent reflections was applied using SADABS.[58] XPREP[59] was used to determine the space group. The structures were solved using SHELXS[60] and refined on all data by full-matrix least-squares with SHELXL-97.[61] Thermal parameters for all non-hydrogen atoms were refined anisotropically. Oak Ridge Thermal Ellipsoid Plot (ORTEP) diagrams were created using ORTEP-32.[62]

Computational Details. All structures and energies were calculated using the Gaussian09 suite of programs.[63] Self-consistent field computations were performed with tight convergence criteria on ultrafine grids, while geometry optimizations were converged to tight geometric convergence criteria for all compounds. Spin expectation values ⟨S⟩^{2} indicated that spin contamination was not significant in any result. Frequencies were calculated analytically at 298.15 K and 1 atm. Structures were considered true minima if they did not exhibit imaginary vibration modes. Optimized geometries were compared using the sum of their electronic and zero-point energies. To reduce the computational time, the isopropyl groups attached to phosphorus were substituted by methyl groups.

The B3LYP hybrid functional was used throughout this computational study.[64,65] For geometry optimizations and frequency calculations, the light atoms were treated with 6-31++G(d,p) basis set,[63] whereas the Ru atoms were treated with ECP28MWB[66] Stuttgart-type basis set.[66,67]

■ ASSOCIATED CONTENT

Ⓢ Supporting Information

Relevant experimental and DFT computational data. This material is available free of charge via the Internet at http://pubs.acs.org.

■ AUTHOR INFORMATION

Corresponding Author

*E-mail: arnold@berkeley.edu.

Notes

The authors declare no competing financial interest.

■ ACKNOWLEDGMENTS

We thank the National Science Foundation for funding (Grant 0848931), Drs. A. DiPasquale, and C. Canlas for experimental assistance, and Ashleigh Ward, Daniel Kellenberger, Henry Storms LaPierre, and Thomas Gianetti for helpful discussions.

■ REFERENCES

(1) Hidai, M.; Mizobe, Y. *Chem. Rev.* **1995**, *95*, 1115−1133.
(2) Howard, J. B.; Rees, D. C. *Chem. Rev.* **1996**, *96*, 2965−2982.
(3) MacKay, B. A.; Fryzuk, M. D. *Chem. Rev.* **2004**, *104*, 385−401.
(4) Hazari, N. *Chem. Soc. Rev.* **2010**, *39*, 4044−4056.
(5) Rodriguez, M. M.; Bill, E.; Brennessel, W. W.; Holland, P. L. *Science* **2011**, *334*, 780−783.
(6) Nishibayashi, Y. *Dalton Trans.* **2012**, DOI: 10.1039/c2dt30105a.
(7) Somorjai, G. A. *Chem. Rev.* **1996**, *96*, 1223−1235.
(8) Crossland, J. L.; Tyler, D. R. *Coord. Chem. Rev.* **2010**, *254*, 1883−1894.
(9) Tuczek, F.; Horn, K. H.; Lehnert, N. *Coord. Chem. Rev.* **2003**, *245*, 107−120.
(10) Barney, B. M.; Lee, H. I.; Dos Santos, P. C.; Hoffmann, B. M.; Dean, D. R.; Seefeldt, L. C. *Dalton Trans.* **2006**, 2277−2284.
(11) Hendrich, M. P.; Gunderson, W.; Behan, R. K.; Green, M. T.; Mehn, M. P.; Betley, T. A.; Lu, C. C.; Peters, J. C. *Proc. Natl. Acad. Sci. U.S.A.* **2006**, *103*, 17107−17112.
(12) Howard, J. B.; Rees, D. C. *Proc. Natl. Acad, Sci. U.S.A.* **2006**, *103*, 17088−17093.
(13) Einsle, O.; Tezcan, F. A.; Andrade, S. L. A.; Schmid, B.; Yoshida, M.; Howard, J. B.; Rees, D. C. *Science* **2002**, *297*, 1696−1700.
(14) Leigh, G. J. *Science* **2003**, *301*, 55−56.
(15) Arashiba, K.; Miyake, Y.; Nishibayashi, Y. *Nat. Chem.* **2011**, *3*, 120−125.
(16) Yandulov, D. V.; Schrock, R. R. *Science* **2003**, *301*, 76−78.
(17) Lukoyanov, D.; Dikanov, S. A.; Yang, Z. Y.; Barney, B. M.; Samoilova, R. I.; Narasimhulu, K. V.; Dean, D. R.; Seefeldt, L. C.; Hoffman, B. M. *J. Am. Chem. Soc.* **2011**, *133*, 11655−11664.
(18) Pool, J. A.; Lobkovsky, E.; Chirik, P. J. *Nature* **2004**, *427*, 527−530.
(19) Demadis, K. D.; Coucouvanis, D. *Inorg. Chem.* **1994**, *33*, 4195−4197.
(20) Demadis, K. D.; Malinak, S. M.; Coucouvanis, D. *Inorg. Chem.* **1996**, *35*, 4038−4046.
(21) Takei, L.; Dohki, K.; Kobayashi, K.; Suzuki, T.; Hidai, M. *Inorg. Chem.* **2005**, *44*, 3768−3770.
(22) Coucouvanis, D.; Demadis, K. D.; Malinak, S. M.; Mosier, P. E.; Tyson, M. A.; Laughlin, L. J. *J. Mol. Catal. A: Chem.* **1996**, *107*, 123−135.
(23) Coucouvanis, D.; Mosier, P. E.; Demadis, K. D.; Patton, S.; Malinak, S. M.; Kim, C. G.; Tyson, M. A. *J. Am. Chem. Soc.* **1993**, *115*, 12193−12194.
(24) Challen, P. R.; Koo, S. M.; Kim, C. G.; Dunham, W. R.; Coucouvanis, D. *J. Am. Chem. Soc.* **1990**, *112*, 8606−8607.
(25) Malinak, S. M.; Demadis, K. D.; Coucouvanis, D. *J. Am. Chem. Soc.* **1995**, *117*, 3126−3133.
(26) Schrock, R. R.; Glassman, T. E.; Vale, M. G. *J. Am. Chem. Soc.* **1991**, *113*, 725−726.
(27) Schrock, R. R.; Glassman, T. E.; Vale, M. G.; Kol, M. *J. Am. Chem. Soc.* **1993**, *115*, 1760−1772.
(28) Collman, J. P.; Hutchison, J. E.; Ennis, M. S.; Lopez, M. A.; Guilard, R. *J. Am. Chem. Soc.* **1992**, *114*, 8074−8080.
(29) Askevold, B.; Nieto, J. T.; Tussupbayev, S.; Diefenbach, M.; Herdtweck, E.; Holthausen, M. C.; Schneider, S. *Nat. Chem.* **2011**, *3*, 532−537.
(30) Arashiba, K.; Sasaki, K.; Kuriyama, S.; Miyake, Y.; Nakanishi, H.; Nishibayashi, Y. *Organometallics* **2012**, *31*, 2035−2041.
(31) Chen, Y. H.; Zhou, Y. H.; Chen, P. P.; Tao, Y. S.; Li, Y.; Qu, J. P. *J. Am. Chem. Soc.* **2008**, *130*, 15250−15251.
(32) Luo, Y.; Li, Y.; Yu, H.; Zhao, J. F.; Chen, Y. H.; Hou, Z. M.; Qu, J. P. *Organometallics* **2012**, *31*, 335−344.
(33) Smith, B. E. *Science* **2002**, *297*, 1654−1655.
(34) Dos Santos, P. C.; Igarashi, R. Y.; Lee, H. I.; Hoffman, B. M.; Seefeldt, L. C.; Dean, D. R. *Acc. Chem. Res.* **2005**, *38*, 208−214.
(35) Zdilla, M. J.; Verma, A. K.; Lee, S. C. *Inorg. Chem.* **2008**, *47*, 11382−11390.
(36) Barney, B. M.; Igarashi, R. Y.; Dos Santos, P. C.; Dean, D. R.; Seefeldt, L. C. *J. Biol. Chem.* **2004**, *279*, 53621−53624.
(37) Barney, B. M.; Yang, T. C.; Igarashi, R. Y.; Dos Santos, P. C.; Laryukhin, M.; Lee, H. I.; Hoffman, B. M.; Dean, D. R.; Seefeldt, L. C. *J. Am. Chem. Soc.* **2005**, *127*, 14960−14961.
(38) Lovell, T.; Li, J.; Liu, T. Q.; Case, D. A.; Noodleman, L. *J. Am. Chem. Soc.* **2001**, *123*, 12392−12410.
(39) Sellmann, D.; Hille, A.; Heinemann, F. W.; Moll, M.; Reiher, M.; Hess, B. A.; Bauer, W. *Chem.—Eur. J.* **2004**, *10*, 4214−4224.
(40) Crossland, J. L.; Balesdent, C. G.; Tyler, D. R. *Inorg. Chem.* **2012**, *51*, 439−445.
(41) Saouma, C. T.; Moore, C. E.; Rheingold, A. L.; Peters, J. C. *Inorg. Chem.* **2011**, *50*, 11285−11287.
(42) Saouma, C. T.; Kinney, R. A.; Hoffman, B. M.; Peters, J. C. *Angew. Chem., Int. Ed.* **2011**, *50*, 3446−3449.
(43) Moret, M. E.; Peters, J. C. *J. Am. Chem. Soc.* **2011**, *133*, 18118−18121.
(44) Chomitz, W. A.; Arnold, J. *Chem.—Eur. J.* **2009**, *15*, 2020−2030.
(45) Rozenel, S. S.; Kerr, J. B.; Arnold, J. *Dalton Trans.* **2011**, *40*, 10397−10405.
(46) Kaess, M.; Friedrich, A.; Drees, M.; Schneider, S. *Angew. Chem., Int. Ed.* **2009**, *48*, 905−907.
(47) Takei, I.; Nishibayashi, Y.; Ishii, Y.; Mizobe, Y.; Uemura, S.; Hidai, M. *J. Organomet. Chem.* **2003**, *679*, 32−42.
(48) Major, Q.; Lough, A. J.; Gusev, D. G. *Organometallics* **2005**, *24*, 2492−2501.
(49) Kuwata, S.; Mizobe, Y.; Hidai, M. *Inorg. Chem.* **1994**, *33*, 3619−3620.
(50) Chaney, A. L.; Marbach, E. P. *Clin. Chem.* **1962**, *8*, 130−132.
(51) Gelabert, R.; Moreno, M.; Lluch, J. M.; Lledos, A.; Pons, V.; Heinekey, D. M. *J. Am. Chem. Soc.* **2004**, *126*, 8813−8822.
(52) Funaioli, T.; Marchetti, F.; Fachinetti, G. *Angew. Chem., Int. Ed.* **2002**, *41*, 3905−3907.
(53) Goicoechea, J. M.; Mahon, M. F.; Whittlesey, M. K.; Kumar, P. G. A.; Pregosin, P. S. *Dalton Trans.* **2005**, 588−597.
(54) Alaimo, P. J.; Peters, D. W.; Arnold, J.; Bergman, R. G. *J. Chem. Educ.* **2001**, *78*, 64−64.
(55) Watt, G. W.; Chrisp, J. D. *Anal. Chem.* **1952**, *24*, 2006−2008.
(56) *SMART, Area-Detector Software Package*; Bruker Analytical X-ray Systems, Inc.: Madison, WI, 2001−2003.

(57) *SAINT SAX Area-Detector Integration Program*, V6.40; Bruker Analytical X-ray Systems Inc.: Madison, WI, 2003.
(58) *SADABS, Bruker-Nonius Area Detector Scaling and Absorption*, v. 2.05; Bruker Analytical X-ray Systems, Inc.: Madison, WI, 2003.
(59) *PREP (v 6.12) Part of the SHELXTL Crystal Structure Determination Package*; Bruker Analytical X-ray Systems, Inc.: Madison, WI, 2001.
(60) *SHELXL Program for the Refinement of X-ray Crystal Structures, Part of the SHELXT Crystal Structure Determination Package*; Bruker Analytical Systems Inc.: Madison, WI, 1995−1999.
(61) *SHELXS Program for the Refinement of X-ray Crystal Structures, Part of the SHELXTL Crystal Structure Determination Package*; Bruker Analytical X-ray Systems Inc.: Madison, WI, 1995−1999.
(62) Farrugia, L. *J. Appl. Crystallogr.* **1997**, *30*, 565.
(63) Frisch, M. J. T., G. W.; Schlegel, H. B.; Scuseria, G. E.; Robb, M. A.; Cheeseman, J.; R.; Scalmani, G. B., V.; Mennucci, B.; Petersson, G. A.; Nakatsuji, H.; Caricato, M.; Li,; X.; Hratchian, H. P. I., A. F.; Bloino, J.; Zheng, G.; Sonnenberg, J. L.; Hada, M.; Ehara,; M.; Toyota, K. F., R.; Hasegawa, J.; Ishida, M.; Nakajima, T.; Honda, Y.; Kitao, O.; Nakai, H. V., T.; J. A. Montgomery, J.; Peralta, J. E.; Ogliaro, F.; Bearpark, M.; Heyd, J. J.; Brothers, E. K., K. N.; Staroverov, V. N.; Kobayashi, R.; Normand, J.; Raghavachari, K.; Rendell, A. B., J. C.; Iyengar, S. S.; Tomasi, J.; Cossi, M.; Rega, N.; Millam, J. M.; Klene,; M.; Knox, J. E. C., J. B.; Bakken, V.; Adamo, C.; Jaramillo, J.; Gomperts, R.; Stratmann, R.; E.; Yazyev, O. A. A. J.; Cammi, R.; Pomelli, C.; Ochterski, J. W.; Martin, R. L.; Morokuma, K. Z. V. G.; Voth, G. A.; Salvador, P.; Dannenberg, J. J.; Dapprich, S.; Daniels, A. D. F. Ö.; Foresman, J. B.; Ortiz, J. V.; Cioslowski, J.; Fox, D. J. *Gaussian09*, Revision B.01; Gaussian, Inc.: Wallingford, CT, 2010.
(64) Becke, A. D. *Phys. Rev. A* **1988**, *38*, 3098−3100.
(65) Lee, C. T.; Yang, W. T.; Parr, R. G. *Phys. Rev. B* **1988**, *37*, 785−789.
(66) Andrae, D.; Haussermann, U.; Dolg, M.; Stoll, H.; Preuss, H. *Theor. Chim. Acta* **1990**, *77*, 123−141.
(67) Martin, J. M. L.; Sundermann, A. *J. Chem. Phys.* **2001**, *114*, 3408−3420.